Bioactive Materials 6 (2021) 1676–1688

Contents lists available at ScienceDirect

Bioactive Materials

journal homepage: www.sciencedirect.com/journal/bioactive-materials

The protective effect of tetrahedral framework nucleic acids on periodontium under inflammatory conditions

Mi Zhou [a,1], Shaojingya Gao [a,1], Xiaolin Zhang [a], Tianxu Zhang [a], Tao Zhang [a], Taoran Tian [a], Songhang Li [a], Yunfeng Lin [a,b], Xiaoxiao Cai [a,*]

[a] State Key Laboratory of Oral Diseases, National Clinical Research Center for Oral Diseases, West China Hospital of Stomatology, Sichuan University, Chengdu, 610041, China

[b] College of Biomedical Engineering, Sichuan University, Chengdu, 610041, China

ARTICLE INFO

Keywords:
tFNAs
Periodontitis
Nanomaterials
Anti-Inflammation
DNA nanotechnology
PDLSCs

ABSTRACT

Periodontitis is a common disease that causes periodontium defects and tooth loss. Controlling inflammation and tissue regeneration are two key strategies in the treatment of periodontitis. Tetrahedral framework nucleic acids can modulate multiple biological behaviors, and thus, their biological applications have been widely explored. In this study, we investigated the effect of tFNAs on periodontium under inflammatory conditions. Lipopolysaccharide and silk ligature were used to induce inflammation *in vivo* and *in vitro*. The results displayed that tFNAs decreased the release of pro-inflammatory cytokines and levels of cellular reactive oxygen species in periodontal ligament stem cells, which promoted osteogenic differentiation. Furthermore, animal experiments showed that tFNAs ameliorated the inflammation of the periodontium and protect periodontal tissue, especially reducing alveolar bone absorption by decreasing inflammatory infiltration and inhibiting osteoclast formation. These findings suggest that tFNAs can significantly improve the therapeutic effect of periodontitis and have the great potential significance in the field of periodontal tissue regeneration.

1. Introduction

Periodontitis is a very common inflammatory disease stimulated by plaque, which can cause inflammatory periodontal bone tissue resorption, potentially lead to tooth loss if left untreated, and tremendously affect the quality of life of patients [1–3]. In addition, it can release numerous inflammatory factors into the blood circulation or cause odontogenic bacteremia, which, in turn, could cause or aggravate chronic inflammation of multiple systemic diseases, such as chronic kidney disease, cardiovascular disease, and diabetes [4,5]. Some studies have demonstrated that the treatment of periodontitis could improve the recovery of systemic diseases, which highlights the therapeutic value of periodontitis treatment [6,7]. The two key treatment objectives for periodontitis are to control inflammation and promote periodontal tissue regeneration, especially alveolar bone regeneration. There are multiple interventions for controlling inflammation, such as tooth scaling, periodontal bag flush, and root planning. In addition, guided tissue regeneration, conventional antibiotics, periodontal bone graft, and growth factors are usually performed by clinicians to regenerate the periodontal tissue [8]. However, the results of these procedures are variable and unsatisfactory [9–11]. Although there are many ways to treat periodontitis, only through a single way can't get a satisfactory therapeutic effect. Therefore, it often requires multiple methods of combined treatment. But, there are still many problems that can't be ignored, such as large trauma, long treatment cycle, uncertain efficacy, etc. Notably, with the rapid development of material science, there has been an attempt to use novel nano-biomaterials to control inflammation and protect damaged periodontal tissue.

Many pathogenic bacteria permanently located in the oral cavity may trigger host inflammation, destroy periodontal tissue homeostasis, and cause periodontitis [12]. In the pathogenesis of periodontal disease, cells around periodontal tissue are exposed to exogenous inflammatory factors such as lipopolysaccharide (LPS) during bacterial infection. These produce endogenous pro-inflammatory factors, which damage the periodontal tissue, especially by causing the resorption of the alveolar bone [13,14]. As one of the most common periodontal adult stem cells,

Peer review under responsibility of KeAi Communications Co., Ltd.

* Corresponding author.
E-mail address: xcai@scu.edu.cn (X. Cai).

[1] Mi Zhou and Shaojingya Gao contributed equally to this work.

https://doi.org/10.1016/j.bioactmat.2020.11.018
Received 19 October 2020; Received in revised form 4 November 2020; Accepted 12 November 2020

periodontal ligament stem cells (PDLSCs) can be induced in different environments to form different tissues such as cementoid tissue, osteoid tissue, and periodontal ligament-like connective tissue. This multi-lineage differentiation potential is not found in other mesenchymal stem cells, and hence, it is regarded as a unique feature of PDLSCs [15]. Therefore, PDLSCs are considered ideal seeding cells to achieve real periodontium regeneration in periodontal tissue engineering. However, the existence of an inflammatory microenvironment is an enormous threat to periodontium regeneration because pro-inflammatory cytokines cannot only aggravate periodontal tissue destruction but also have a negative influence on periodontium regeneration by downregulating the osteogenic differentiation and migration of PDLSCs [16,17]. Hence, the control of inflammation is important for periodontal tissue regeneration.

As a novel nucleic acid, tetrahedral framework nucleic acid (tFNA), also known as tetrahedral DNA nanostructure (TDN), is significant in structural DNA nanotechnology due to its unique biological, chemical, and physical properties [18,19]. tFNA is composed of four prefabricated single-strand DNA (ssDNA); it is regarded as the most practical FNA and widely used for biological applications, such as drug delivery, biosensing, imaging, and intelligent membrane engineering [20,21]. In addition, tFNAs have potential to regulate the biological behaviors of multiple cells such as adipose and neural stem cells, which are also used in tissue engineering [22,23].

Recent evidence suggests that tFNA can facilitate the proliferation and osteo/odontogenic differentiation of odontogenic stem cells such as DPSCs and PDLSCs in a normal environment [24,25]. In addition, tFNA possesses excellent anti-oxidation and anti-inflammatory properties mediated by the modulation of macrophage response through the inhibition of MAPK phosphorylation [26]. As the critical factors of the MAPK/ERK signaling pathway, P38, JNK, and ERK can be activated by environmental stress, inflammatory cytokines, and G protein-coupled receptor to induce inflammation [27]. Therefore, this study determined if tFNA, under inflammatory conditions *in vitro* and *in vivo,* could inhibit the release of inflammatory cytokines, upregulate the osteogenic differentiation of PDLSCs by attenuating MAPK/ERK phosphorylation, and protect the periodontal tissue by inhibiting inflammation in periodontitis.

2. Materials and methods

2.1. Synthesis of tFNAs

The synthesis of tFNAs was performed according to the procedure described in previous studies (Table 1). [28,29] The four well-defined DNA single strands were added in TM buffer, which were denatured at 95 °C and annealed at 4 °C.

2.2. Characterization of tFNAs

Transmission electron microscopy (TEM), capillary electrophoresis, and 8% polyacrylamide gel electrophoresis (PAGE) were used to confirm the successful synthesis of tFNA [30,31]. In addition, the fundamental features of tFNAs were analyzed by dynamic light scattering (Zetasizer Nano ZS90, Malvern Instrument Ltd., Malvern, UK).

2.3. Samples, culture, and treatment of PDLSCs

With informed consent from the donors, the study samples were collected from the third molar teeth of adults aged less than 25 years, which met the requirements of the ethics committee of Sichuan University [32]. PDLSCs were isolated and cultured following the procedure used by Nan Yang and colleagues [33]. For subsequent experiments, the cells were separated into three groups: blank group without lipopolysaccharides (LPS; lipopolysaccharide from *Porphyromonas gingivalis*, InvivoGen, San Diego, CA, USA) and tFNAs; LPS group treated with LPS (2 μg/mL); tFNAs groups incubated with tFNAs (250 nM) for 1 h followed by LPS treatment (2 μg/mL).

2.4. Cellular uptake of tFNAs

To explore if tFNAs could be absorbed by PDLSCs, the cells were exposed to CY5-tFNAs, CY5-ssDNA, and LPS for 6 h. The images of the samples were captured by a confocal laser microscope (A1R MP^{+}, Nikon, Tokyo, Japan).

2.5. Wound healing assay

When the cells reached 90% confluence in 6-well plates, we used sterile pipette tips to create a bidirectional wound by scratching the cells. After washing with PBS, the samples were exposed to tFNAs or LPS with α-MEM containing 1% FBS. Wound healing was recorded at 0, 12, 24, and 36 h after treatment with tFNAs.

2.6. Detection of reactive oxygen species (ROS) level

DCFH-DA assay (Beyotime, Shanghai, China) was used to detect the levels of ROS in PDLSCs. After plating the cells onto 24-well culture dishes (2×10^4/well) overnight, the cells were treated with tFNAs or LPS for 6 h, followed by incubation with a DCFH-DA probe for 20 min. To locate the cell nucleus, Hoechst 33342 solution (Beyotime, Shanghai, China) was used to stain the live cells. Finally, the sample images were captured using an inverted fluorescence microscope (DMi8, Leica, Wetzlar, Germany).

2.7. Quantitative polymerase chain reaction (qPCR)

To assess the gene expression of osteogenic-related factors such as runt-related transcription factor 2 (RUNX2), ALP, and osteopontin (OPN) under inflammatory conditions, quantitative polymerase chain reaction (qPCR) was applied. The sequences of forward and reverse primers of these genes are displayed in Table 2. After treatment with tFNAs or LPS for 1 day, gene samples were extracted using TRIzol reagent (Thermo Fisher Scientific, MA, USA). To purify and obtain the cDNA, we employed a cDNA synthesis kit (Mbi, Glen Burnie, MD, USA). SYBR Green I PCR master mix and Bio-Rad real-time PCR system (Bio-Rad, Hercules, CA, USA) were used to perform qPCR [34].

Table 1
Base sequence of each single-stranded DNA (ssDNA).

ssDNA	Direction	Base Sequence
S1	5′→3	ATTTATCACCCGCCATAGTAGACGTATCACCAG GCAGTTGAGACGAACATTCCTAAGTCTGAA
S2	5′→3′	ACATGCGAGGGTCCAATACCGACGATTACAGCT TGCTACACGATTCAGACTTAGGAATGTTCG
S3	5′→3′	ACTACTATGGCGGGTGATAAAACGTGTAGCAAGC TGTAATCGACGGGAAGAGCATGCCCATCC
S4	5′→3′	ACGGTATTGGACCCTCGCATGACTCAACTGCCTGGTGATACGAGGATGGGCATGCTCTTCCCG
cy5-S1	5′→3′	cy5-ATTTATCACCCGCCATAGTAGACGTATCACCAGGCAGTT GAGACGAACATTCCTAAGTCTGAA

Table 2
Sequences of forward and reverse primers of selected genes designed for q-PCR.

Gene	Direction	Sequence
GAPDH	5′-3′	CAGGGCTGCTTTTAACTCTGG
	3′-5′	TGGGTGGAATCATATTGGAACA
RUNX2	5′-3′	TGGTTACTGTCATGGCGGGTA
	3′-5′	TCTCAGATCGTTGAACCTGCTA
ALP	5′-3′	ACTGGTACTCAGACAACGAGAT
	3′-5′	ACGTCAATGTCCCTGATGTTATG

2.8. Western blotting

To explore the effect of tFNAs on inflammation, the associated mechanism, and osteogenic differentiation under inflammatory conditions, the protein expression of pro-inflammatory factors was determined by western blotting. Furthermore, the release of the vital factors of the MAPK/ERK signaling pathway, as well as that of OPN and RUNX2 were also determined. Except for the samples of OPN and Runx2 treated with tFNAs for 3 days, the other protein samples were exposed to tFNAs for 24 h. All samples were isolated by the cell protein extraction reagent (KeyGen Biotech, Nanjing, China). Anti-IL6 (1:2000, Abcam, Cambridge, England), anti-IL-1β (1:2000, Abcam, Cambridge, England), anti-TNF-α (1:2000, Abcam, Cambridge, England), anti-p38 (1:2000, Abcam, Cambridge, England), anti-p-p38 (1:2000, Abcam, Cambridge, England), anti-ERK1/2 (1:2000, Abcam, Cambridge, England), anti-p-ERK1/2 (1:2000, Abcam, Cambridge, England), anti-JNK1/2/3 (1:2000, Abcam, Cambridge, England), anti-p-JNK1/2/3 (1:2000, Abcam, Cambridge, England), anti-OPN (1:2000, Abcam, Cambridge, England) and anti-Runx2 (1:2000, Abcam, Cambridge, England) primary antibodies were incubated with the protein samples overnight. Next, the secondary antibody (Beyotime, Shanghai, China) was chose to incubate the samples for 60 min, and the ECL chemiluminescence detection system (Bio-Rad, Hercules, CA, USA) was performed to detect the protein bands.

2.9. Immunofluorescence

To verify the results of western blotting, we plated the PDLSCs in 12-well plates (2×10^4/well) to perform immunofluorescence staining. After 1 day or 3 days of treatment, PDLSCs were fixed with 4% (v/v) paraformaldehyde, followed by incubation with 0.5% Triton X-100 and 5% goat serum. Related primary antibodies (1:200–1:300; anti-TNF-α, anti-IL-1β, anti-IL6, anti-OPN, and anti-Runx2) were incubated with the samples overnight. After that, the cells were incubated with DyLight 488 secondary antibody (1:400; Thermo Fisher Scientific, MA, USA) to conjugate with fluorescence before staining with FITC-labeled phalloidin and DAPI. Subsequently, cell morphology and the intensity of protein fluorescence were observed using a confocal laser microscope (A1R MP^+, Nikon, Japan).

2.10. Experimental animals

All animals used in this study were Sprague-Dawley male rats aged 8–10 weeks. The animal experiments were approved by the ethics committee of Sichuan University.

2.11. Ligature-induced periodontitis models

The maxillary left second molar of the rat was ligated with a 3-0 silk suture for 3 weeks, and the contralateral molar tooth was untreated as the blank control group [35]. During ligation, the tFNA or saline solution (20 μL) was injected into the gingival sulcus every other day.

2.12. Histology

The left maxillae were conventionally fixed with 4% PFA, decalcified with EDTA, embedded in paraffin, and cut into sections in the midsagittal plane of the second molar. These samples were subjected to tartrate-resistant acid phosphatase (TRAP) staining, Masson stain, as well as hematoxylin and eosin (H&E) staining.

2.13. TRAP staining

A high level of pro-inflammatory cytokines is released into the periodontium in periodontitis, and they could activate osteoclastogenesis, enlarge the function of osteoclasts, and restrain the activity of osteoblasts, leading to excessive resorption of alveolar bone. Therefore, we aimed to explore the level of osteoclast activity by using TRAP staining. The positive cells in the furcation region were observed with the Aperio Imagescope software (Aperio Technologies, Inc., CA, USA) at 5 × magnification, and 20 × magnification. The cytoplasm of the osteoclasts was dark red, and the nucleus was blue.

2.14. Immunohistochemistry

After sealed by 3% hydrogen peroxide, the slices were incubated with anti-IL6 (1:500, Serviceblo, Wuhan, China), anti-IL-1β (1:800, Serviceblo, Wuhan, China) primary antibodies overnight. After that, the secondary antibodies (Serviceblo, Wuhan, China) were chose to incubate the samples for 50 min. The slices were stained by hematoxylin (Serviceblo, Wuhan, China) and diaminobenzidine (Serviceblo, Wuhan, China), which was visualized by microscopic analysis.

2.15. Micro-computed tomography (Micro-CT) analysis

As a nondestructive three-dimensional (3D) imaging technology, micro-CT can clearly understand the internal microstructure of a sample without destroying the sample, and hence, it is applied to observe small changes in the alveolar bone. After fixation with 4% paraformaldehyde and immersion in 70% ethanol, the maxillary left alveolar bone of the rats was scanned with a micro-CT (μCT 50, SCANCO Medical AG, Switzerland) under the following conditions: 10 μm pixel size and 70 kV X-ray energy. Scanned data were evaluated and reconstructed using the SCANCO Medical Evaluation software.

On the sagittal plane, the CEJ-ABC distance (the distance between the cementoenamel junction and alveolar bone crest) of the second molar was measured as the distal, middle, and mesial bone resorption. The alveolar bone between two buccal roots underneath the second molar was drawn as the region of interest (ROI) for bone volume measurement, which consisted of 50 2D slices. The ratio of bone volume to tissue volume (BV/TV), trabecular thickness (Tb.Th), trabecular separation/space (Tb.Sp), and trabecular number (Tb.N)for the ROI were measured by the micro-computed tomography evaluation program (V6.5-3, Switzerland).

2.16. Statistical analysis

t-test or one-way ANOVA in GraphPad Prism 6.01 (GraphPad Software Inc., San Diego, CA, USA) was used to perform the statistical evaluation. All experiments were carried out at least three times.

3. Results

3.1. Characterization of tFNAs

Fig. 1 displays some of the main characteristics of tFNAs, such as the morphology and average size. As shown in Fig. 1a, four ssDNAs (Table 1) were added in equal proportion to synthesize tFNA according to the principle of complementary base pairing. Fig. 1b displays the TEM

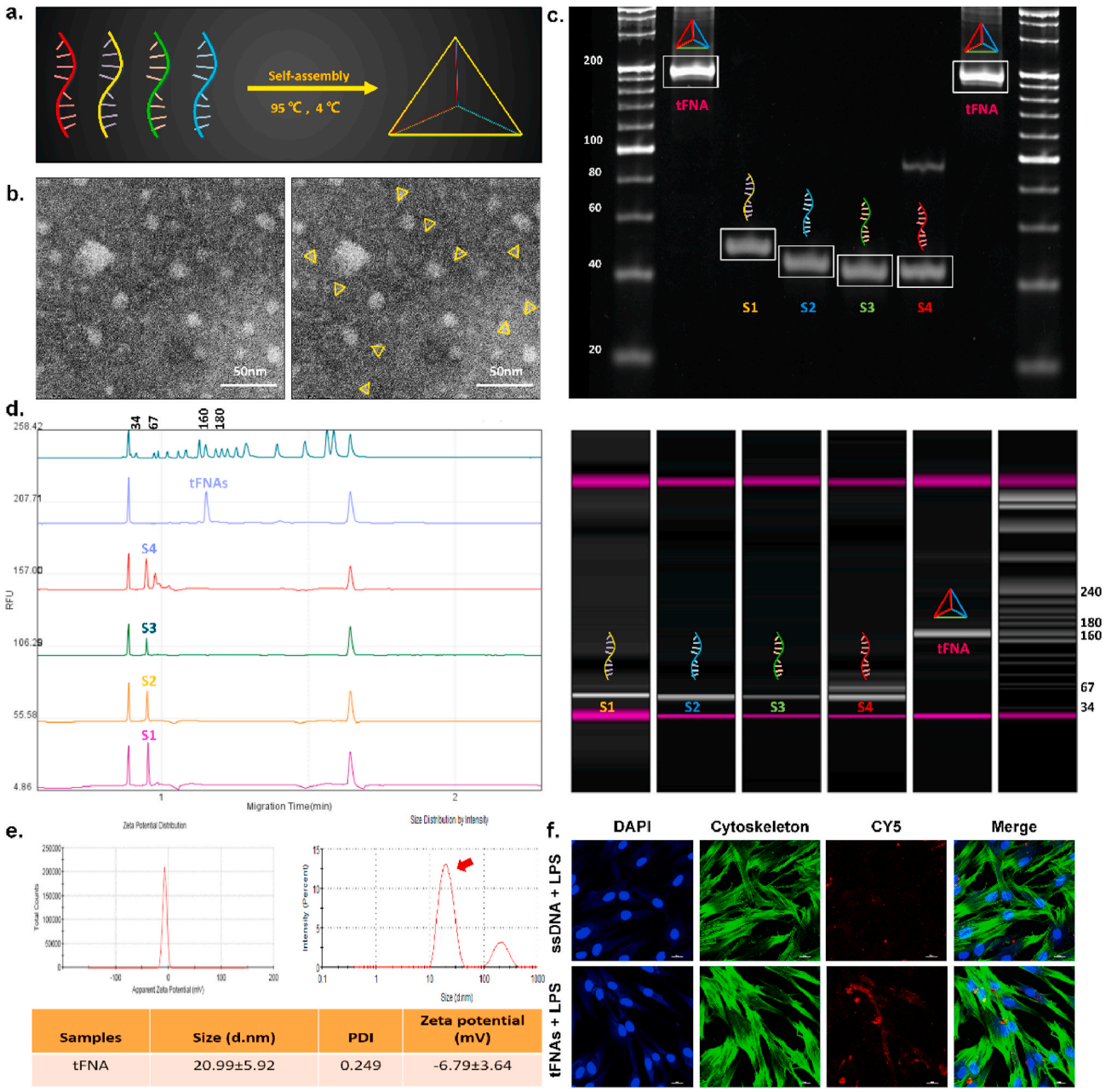

Samples	Size (d.nm)	PDI	Zeta potential (mV)
tFNA	20.99±5.92	0.249	-6.79±3.64

Fig. 1. Synthesis and characterizations of tFNAs. a. A structure diagram displaying the composition of tFNAs. b. The images of transmission electron microscope showing the morphology and the average size of tFNAs. Scale bars are 50 nm. c. The result of 8% Polypropylene Acyl Amine Gel Electrophoresis demonstrating the successful production of tFNAs. d. The result of capillary electrophoresis demonstrating the successful production of tFNAs. e. Size distribution and Zeta potential test of tFNAs. f. The cellular uptake of CY5-tFNAs was explored by immunofluorescence staining. (nucleus: blue, cytoskeleton: green, cy5: red). Scale bars are 25 μm.

images, from which we could see some triangular nanoparticles. The results obtained from 8% SDS-PAGE and capillary electrophoresis demonstrated the successful synthesis of tFNAs (Fig. 1c, d). Dynamic light scattering was employed to explore the zeta potential and average size of tFNA. Fig. 1e shows the average size of tFNA was about 20.99 nm and the average zeta potential was approximately −6.79 mV.

3.2. Uptake of tFNAs by PDLSCs

Some studies have reported that unlike ssDNA, tFNAs could be largely taken in by some specific cells without the assistance of carriers [36,37]. Therefore, CY5 with a red fluorescence signal was used to tag the S1 and TDNs to explore the uptake of tFNA by PDLSCs. The fluorescence intensity of CY5-tFNAs was significantly stronger than that of CY5–S1 under inflammatory conditions, which indicates that tFNAs could enter PDLSCs in abundance to play diverse roles, but ssDNA could not (Fig. 1f).

3.3. tFNAs promote the migration of PDLSCs under inflammatory conditions

As a widely used method for detecting cell migration ability *in vitro*, a wound healing assay was employed to observe the roles played by tFNAs in PDLSCs in an inflammatory environment. We adopted four time points (0 h, 12 h, 24 h, and 36 h) to explore the migration of cells after treatment. As shown in Fig. 2a, the migration rate of the LPS group was obviously decreased. In addition, the migration rate of the tFNA + LPS group was significantly enhanced in comparison with that of the LPS

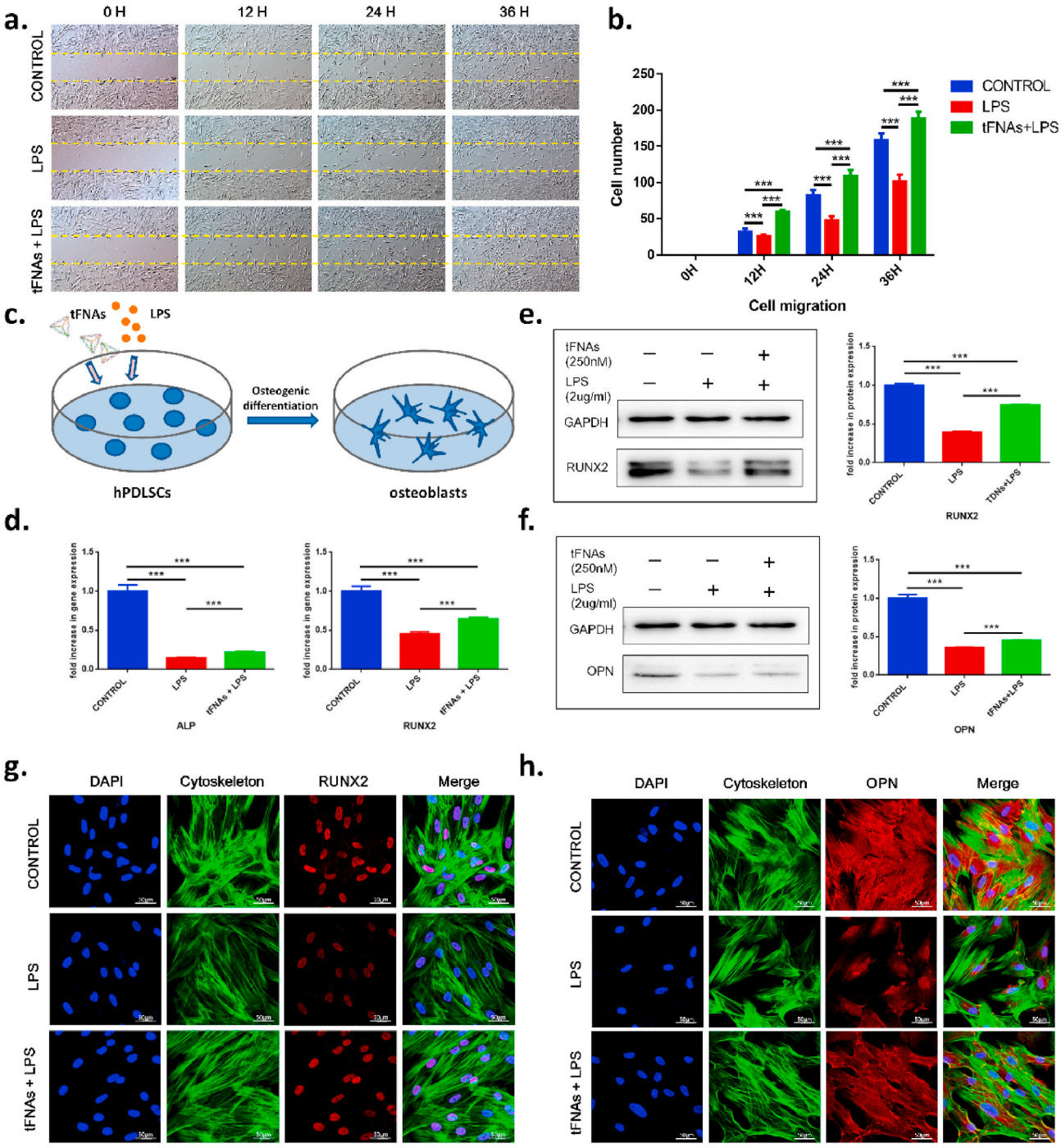

Fig. 2. tFNAs promote the migration and osteogenic differentiation of PDLSCs under inflammatory conditions. a. The images of wound healing assay. b. The statistical analysis of wound healing assay. Data are presented as means ± standard deviations (n = 3). ***P < 0.001. c. The schematic diagram of tFNAs promoting osteogenic differentiation of PDLSCs in an inflammatory microenvironment. d. Treated with tFNAs and LPS, the statistical analysis of the result of Q-PCR. Data are presented as means ± standard deviations (n = 3). ***P < 0.001. e. The WB result of RUNX2 protein and the statistical analysis of WB result after exposed to tFNAs and LPS. Data are presented as means ± standard deviations (n = 3). ***P < 0.001. f. The WB result of OPN protein and the statistical analysis of WB result after exposed to tFNAs and LPS. Data are presented as means ± standard deviations (n = 3). ***P < 0.001. g. The expression of osteogenic-related proteins was imaged by immunofluorescence staining. (nucleus: blue, cytoskeleton: green, RUNX2 protein: red). Scar bars are 25 μm. h. The expression of osteogenic-related proteins was imaged by immunofluorescence staining. (nucleus: blue, cytoskeleton: green, OPN protein: red). Scar bars are 25 μm.

group, with the rate even faster than that of the control group. The statistical analysis of the migration volume revealed that LPS-induced inflammation decreased the migration of PDLSCs, but tFNAs significantly upregulated cell stability (Fig. 2b).

3.4. tFNAs promote osteogenic differentiation of PDLSCs under inflammatory conditions

As reported previously, tFNAs could upregulate the osteogenic differentiation of some cells such as ASCs and DPSCs under regular conditions [24,38]. In addition, the osteogenic capacity of PDLSCs would be

highly damaged under an inflammatory environment. Therefore, we explored the effect of tFNAs on the osteogenic differentiation of PDLSCs under inflammatory conditions as Fig. 2c. Using qPCR, we determined the gene expression of ALP and RUNX 2 in PDLSCs incubated with tFNAs for 24 h. The results showed that the addition of LPS to induce an inflammatory environment inhibited the expression of ALP and RUNX 2, whereas treatment with tFNAs enhanced the expression of the genes (Fig. 2d).

To verify the protective effect of tFNAs, the protein expression of osteogenic factors such as OPN and RUNX2 was measured by western blotting and immunofluorescence staining. As displayed by the protein bands, the expression of the proteins in LPS group was greatly decreased, whereas that in the tFNA + LPS group increased under inflammatory conditions (Fig. 2e, f). In addition, immunofluorescence staining showed the same trend; the fluorescence intensity of OPN and RUNX 2 proteins were downregulated by LPS but upregulated by tFNAs (Fig. 2g, h). Therefore, inflammation has inhibitory effect on the osteogenic differentiation of PDLSCs, whereas tFNAs have the ability to enhance the osteogenic capacity.

3.5. The antioxidant and anti-inflammatory effects of tFNAs on PDLSCs

To explore the antioxidant and anti-inflammatory effects of tFNAs on PDLSCs in LPS activated inflammation microenvironment, the experiments *in vitro* were conducted as Fig. 3a.

As a crucial factor of oxidative stress, the overproduction of ROS in cells can cause the destruction of cell membranes and release plenty of mediators to cause inflammation [39]. Therefore, we investigated if tFNAs could reduce ROS production and inhibit LPS-induced inflammation by detecting changes in ROS production using the ROS Assay Kit (Beyotime, Shanghai, China). After incubation with the fluorescent probe DCFH-DA for 20 min, the cells were stained with DCF. Because non-fluorescent DCFH can be oxidized by intracellular ROS to produce DCF with green fluorescence, the level of intracellular ROS could be determined by the intensity of green fluorescence. The fluorescence intensity of the LPS group was much stronger than that of the control group; nevertheless, that of the tFNA + LPS decreased to a level as low as that of the control group (Fig. 3b). Therefore, tFNAs could downregulate intracellular ROS production, which may inhibit inflammation in PDLSCs.

The levels of pro-inflammatory cytokines indicate, to some extent, the degree of inflammation. In addition, some studies reported that the presence of these cytokines could affect several behaviors of PDLSCs, such as migration, and osteogenic differentiation [40,41]. Therefore, we examined if tFNAs could prevent inflammation and reduce the expression of inflammatory factors to protect PDLSCs under inflammatory conditions.

After treatment with tFNAs and LPS, q-PCR, western blotting and immunofluorescence staining were performed to detect the changes in the gene or protein levels of TNF-α, IL-6, and IL-1β in PDLSCs. The

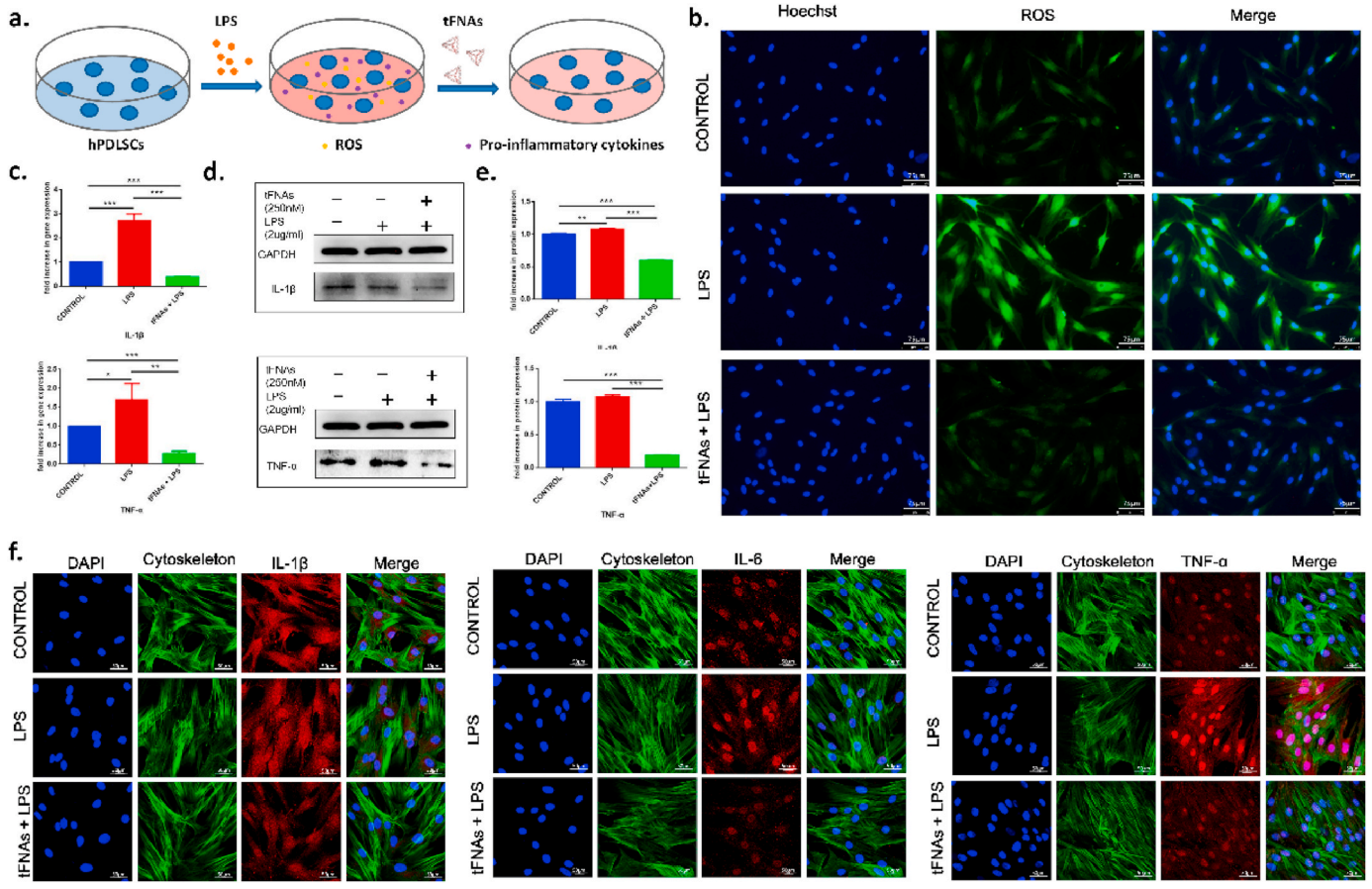

Fig. 3. tFNAs decrease the expression of cellular ROS and pro-inflammatory cytokines of PDLSCs under inflammatory conditions. a. Schematic diagram of the antioxidant and anti-inflammatory effects of tFNAs on PDLSCs under inflammatory conditions. b. The production of cellular ROS induced by LPS was analyzed by inverted fluorescence microscope, which demonstrated that tFNAs decreased the cellular ROS production. Scar bars are 75 μm. c. Treated with tFNAs and LPS, the statistical analysis of the result of Q-PCR. Data are presented as means ± standard deviations (n = 3). ***P < 0.001. d. The WB results of IL-1β and IL-6 with the treatment of tFNAs. e. The statistical analysis of WB result. Data are presented as means ± standard deviations (n = 3). ***P < 0.001. f. The results of immunofluorescence staining displayed that the expression of IL-1β, IL-6 and TNF-α were obviously down-regulated after treatment with tFNAs. (nucleus: blue, cytoskeleton: green, IL-1β/IL-6/TNF-α protein: red). Scar bars are 25 μm.

results of q-PCR showed that the expression of these genes in the positive control group (group tFNA + LPS) was significantly reduced. Moreover, the gene expression in the tFNA + LPS group was even lower than that in the control group (Fig. 3c). In addition, the results of western blotting and immunofluorescence staining displayed the same trend that tFNAs could greatly decrease the protein expression of these factors in inflammatory microenvironment (Fig. 3d, e and 3f). In summary, these results indicate that tFNAs could prevent inflammation and decrease the release of inflammatory factors in PDLSCs.

3.6. Potential mechanism through which tFNAs inhibit the inflammation of PDLSCs

Previous studies have reported that the MAPK/ERK signaling pathway could have a vital impact on the inflammation of PDLSCs [42, 43]. Therefore, the protein levels of ERK, JNK, and P38 (protein kinases considered crucial factors for the MAPK/ERK signaling pathway) were determined by western blotting to explore if tFNAs could prevent the inflammation of PDLSCs by inhibiting the phosphorylation of signaling pathway (Fig. 4a). As Fig. 4b and Fig. 4c shows, the protein level of ERK, JNK, and P38 in the group exposured to tFNAs and LPS was prominently decreased compared with that of the group treated with LPS alone. This indicates that tFNAs protected PDLSCs against inflammation by inhibiting the MAPK/ERK signaling pathway.

3.7. tFNAs inhibit the inflammatory response of periodontitis in vivo

During the development of periodontitis, several inflammatory immune responses occur. Therefore, there is a large amount of infiltrating inflammatory cells and a great release of pro-inflammatory cytokines in the periodontal tissue. In this study, we intended to explore the inflammatory response of periodontitis treated with tFNAs and saline through H&E and immunohistochemical staining for IL-6 and IL-1β as the sketch diagram displayed (Fig. 5a).

The H&E staining in Fig. 5b shows that there was a large amount of infiltrating inflammatory cells in the alveolar bone between the two roots of the second molar of the control group treated with normal saline. However, there was no obvious inflammatory cell infiltration in the experimental group treated with tFNAs, which showed almost the same result as the blank group with healthy periodontal tissue. Fig. 5c and d displays the results of the immunohistochemical staining of IL-6 and IL-1β. As seen in the figures, there was a lot of yellow or brown material accumulation in the control group, which suggests that there was a high level of pro-inflammation factors released in the periodontium. The expression of these cytokines in tFNA (250 nM and 500 nM) groups were markedly decreased as compared to the controls. These findings indicate that tFNAs could significantly inhibit the inflammatory response of periodontitis, which could greatly reduce damage to the periodontal tissue.

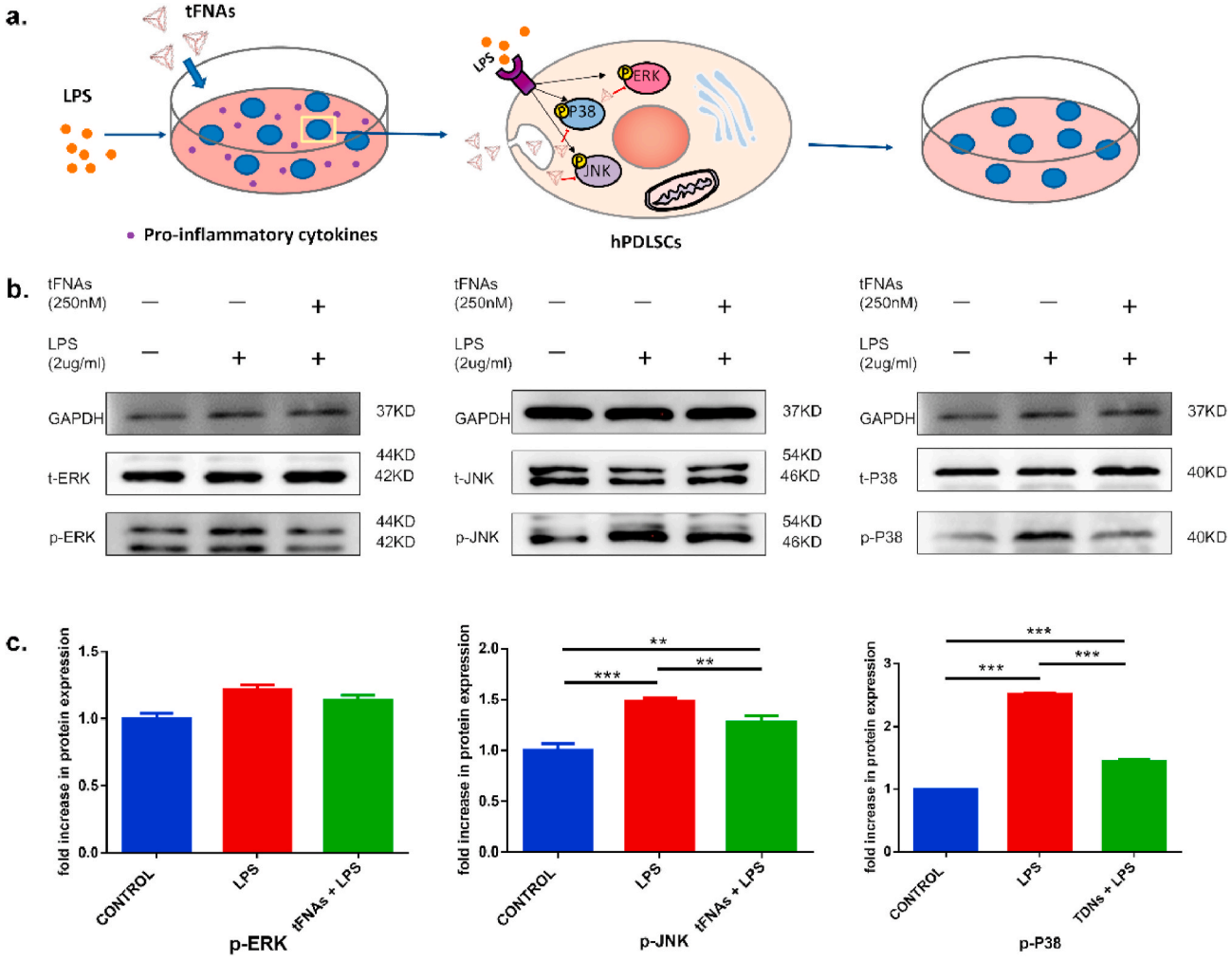

Fig. 4. tFNAs inhibited phosphorylation of MAPK/ERK signaling pathway of PDLSCs in inflammatory microenvironment. a. Schematic diagram of tFNAs inhibiting LPS-induced phosphorylation of ERK, JNK and p38 in PDLSCs. b. WB analysis of total ERK, phosphor-ERK, total JNK and phosphor-JNK, total p38, phosphor-p38 of PDLSCs under inflammatory conditions. c. Statistical analysis of the results of WB. Data are presented as means ± standard deviations (n = 3). ***P < 0.001.

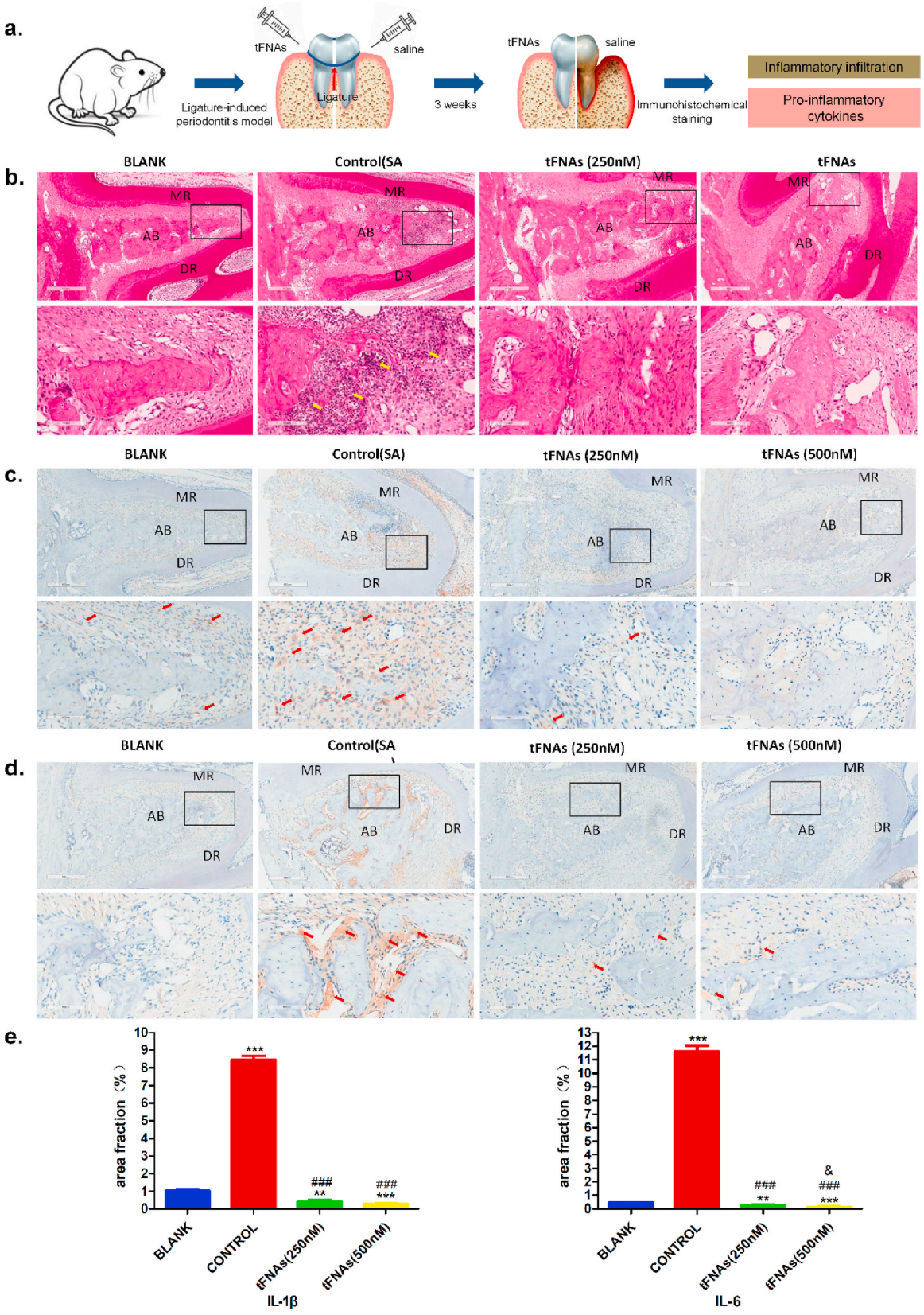

Fig. 5. tFNAs significantly reduced the inflammation of periodontitis *in vivo*. a. Schematic diagram of the rat periodontitis experiment. b. The images of H&E staining at 5 × magnifcation and 20 × magnifcation. The yellow arrow showed the inflammatory cells. c. The immunohistochemical results of IL-1β at 5 × magnifcation and 20 × magnifcation. IL-1β was displayed by the red arrow. d. The immunohistochemical images of IL-6 at 5 × magnifcation and 20 × magnifcation. IL-6 was showed by the red arrow. e. Statistical analysis of expression of IL-1β and IL-6 in periodontal tissue. * *P < 0.01, ***P < 0.001 compared with blank group. ###P < 0.001 compared with contol group. & P < 0.5 compared with tFNAs (250 nM) group. MR/DR = mesial root/distal root; AB = alveolar ridge.

3.8. tFNAs inhibit the destruction of periodontal tissue of periodontitis in vivo

Periodontitis can lead to the destruction of periodontal tissue, such as alveolar bone, cementum, and periodontal ligament. Therefore, we conducted an *in vivo* study to further confirm the intervention or protective effect of tFNAs on periodontal tissues of periodontitis, as shown in the schematic sketch (Fig. 6a).

As the fibrous connective tissue between root and alveolar bone, the matrix and collagen of periodontal ligament (PDL) will degenerate and degrade due to inflammation. In order to explore the histological changes of PDL, Masson staining was applied. Inflammation resulted in a sparse PDL structure and a significant decrease in collagen content in the control group. However, treatment with tFNAs for 3 weeks, the structure of PDL was denser and the amount of collagen fibers increased greatly compared with control group, which was basically the same or even

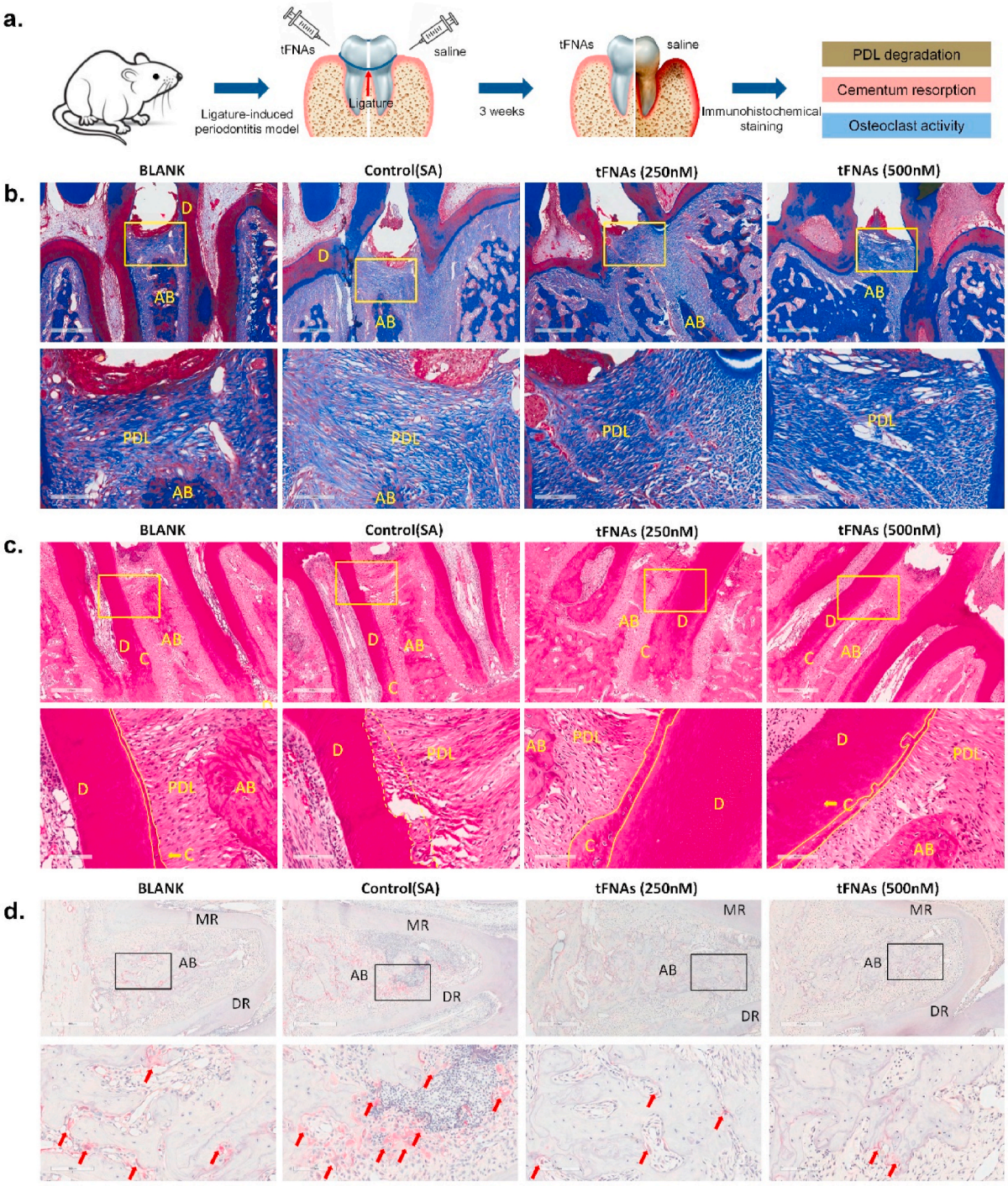

Fig. 6. tFNAs obviously inhibit the destroy of periodontal tissue from periodontitis *in vivo*. a. Schematic diagram of the rat periodontitis experiment. b. The images of Masson staining at 5 × magnifcation and 20 × magnifcation. c. The images of H&E staining at 5 × magnifcation and 20 × magnifcation. The aera surrounded by yellow solid line was cementum, and the aera surrounded by yellow dotted line was the cementum absorbed by inflammation. d. The photographs of TRAP staining at 5 × magnifcation and 20 × magnifcation. The red arrow indicated the osteoclasts. MR/DR = mesial root/distal root; AB = alveolar ridge; D = dentin; C = cementum; PDL = periodontal ligament.

more than the blank group (Fig. 6b).

Cementum is located on the surface of the tooth root and is inserted vertically by the Sharpey fibers. With the development of periodontitis, the cementum will be absorbed. The results of H&E staining displayed that the part marked by the yellow dotted line, including cementum and even dentin, had been absorbed due to inflammation in control (SA) group. In addition, the Sharpey fibers had also undergone denaturation and degradation. However, the use of tFNAs protected the cementum from inflammation, which leaved the cementum and Sharpey fibers almost intact (Fig. 6c).

The absorption of alveolar bone has attracted the most attention. Periodontitis can cause the local resorption of alveolar bone. Previous studies have demonstrated that inflammatory immunological response could promote osteoclastogenesis and restrain osteoblastogenesis, which disrupts the balance of osteoclasts and osteoblasts, thus causing the resorption of bone tissue [44]. This study investigated the activity of osteoclasts and the resorption of alveolar bone in periodontitis.

Osteoclasts were stained dark red and multinuclear by TRAP staining. The number of cells was obviously increased in control group and significantly reduced in tFNA (250 nM and 500 nM) groups (Fig. 6d).

To observe the periodontal bone loss and bone mass, micro-CT analysis was carried out (Fig. 7a). Fig. 7b shows the 3D reconstruction of the maxillary alveolar, which could determine the degree of alveolar bone absorption in each group. The red part displays the level of dental root exposure, which was consistent with the extent of alveolar bone loss after treatment with tFNAs. The result of the quantitative analysis of bone resorption at the three sites of the mesial buccal root, middle buccal root, and distal buccal root in the second molar is shown in Fig. 7c.

Micro-CT images revealed significant dental root exposure in the affected maxillary second molar regions in the control group. However, the tFNA groups (250 nM and 500 nM) displayed a marked decrease in bone resorption. In particular, when the drug concentration was 500 nM, there was no statistical difference between the bone resorption of the treated group and that of the blank group, which means that the tFNA (500 nM) group showed almost no bone resorption.

BV/TV, Tb.Th, Tb.Sp, and Tb.N are common indices of changes in bone mass. High BV/TV, Tb.Th, and Tb.N values indicate high bone mass; however, the smaller the Tb.Sp, the higher the bone density. Therefore, we determined the changes in bone mass by analyzing the changes in these indices. Fig. 7d shows that there was a considerably low BV/TV in the affected maxillary molar regions in the control group. The micro-CT images and the analysis revealed nearly no dental root exposure in the tFNA (500 nM) group. The rats that were treated with 500 nM tFNAs exhibited a higher BV/TV and similar Tb.Sp, Tb.Th, and Tb.N, compared with the blank group. These findings demonstrated that tFNAs have a suitable therapeutic value for periodontitis.

4. Discussion

Periodontal degeneration and periodontium defects caused by microbial-related inflammatory periodontal diseases have affected the vast majority of the population, and they are regarded as a vital public health concern [45]. The current methods of treating periodontitis are mainly divided into three categories, namely basic treatment, medical treatment and surgical treatment. Among them, basic treatment and drug treatment are to remove plaque, kill bacteria, and control inflammation, thereby reducing the damage of inflammation to periodontal tissue. However, drug therapy alone is not the main method for the treatment of periodontitis, only for patients who are ineffective in basic treatment can consider adjuvant medication. Besides that, they are prone to cause bacterial flora imbalance and drug resistance, and the effect of single drug use is not ideal. Therefore, these drugs, such as metronidazole, tetracycline, minocycline gel, etc., must be used as auxiliary drugs for basic treatment to treat periodontitis. Surgical treatment, including bone graft, GBR, GTR, etc., is to promote the regeneration of periodontal tissue, which can reconstruct the tissue defect caused by periodontitis. However, it also has some disadvantages that cannot be ignored, such as large trauma, long treatment cycle, uncertain regeneration effect and so on [9–11]. tFNAs, as novel DNA nanomaterials, can be used locally to treat periodontitis and achieved satisfactory results in this study with the absence of periodontal basic treatment. It has many advantages: good treatment effect, reduced treatment steps (such as no longer need periodontal basic treatment and surgical treatment), minimally invasive, high biological safety, no bacterial imbalance, etc., Therefore, tFNAs is an ideal drug for the treatment of periodontitis to inhibit inflammation, reduce the damage to periodontal tissue, and promote periodontium regeneration.

As a novel nucleic acid nanomaterial, the biological applications of tFNAs have been extensively explored. tFNAs cannot only clear senescent human dermal fibroblasts and facilitate attenuated apoptosis of ASCs but can also promote the wound healing, such as through the up-regulation of corneal transparency to facilitate corneal wound heal [46,47]. In this study, we induced an inflammatory microenvironment *in vitro* with LPS and explored if tFNAs could attenuate the release of pro-inflammatory factors and promote osteogenic differentiation. Treatment with tFNAs decreased the cellular production of IL-6, TNF-α, and IL-1β. In addition, as a mediator of inflammation, the cellular level of ROS of PDLSCs was also significantly downregulated after exposure to tFNAs, which indicates that tFNAs possesses anti-inflammatory properties. Considerable information from the literature suggests that the MAPK/ERK signaling pathway is interrelated with inflammation and can be activated to induce inflammation [40,43]. Therefore, we detected the expression of p-ERK, p-JNK, and p-P38 proteins. The results showed that tFNAs suppressed the activation of the MAPK/ERK signaling pathway by reducing the expression of inflammatory factors, which indicates that tFNAs inhibited the inflammation of PDLSCs through the MAPK/ERK signaling pathway. The existence of inflammatory factors is a great threat to periodontal regeneration, because they cannot only greatly reduce the migration ability of cells, thus hindering the migration of healthy PDLSCs to the bone defect area, but also can down regulate the osteogenic differentiation ability of cells to inhibit periodontal bone regeneration [16,17]. Therefore, tFNAs could up-regulate the migration and osteogenic differentiation of PDLSCs by inhibiting the expression of inflammatory factors and ROS.

For the *in vivo* experiment, 3-0 silk was used to tie up the second molar of Sprague-Dawley rats for 3 weeks to induce periodontitis. Upon treatment with 500 nM tFNAs, the alveolar bone of periodontitis mostly showed no change compared with the normal periodontal tissue, regardless of the height or density. In addition, the number of osteoclasts, inflammatory infiltration, and the levels of IL-6 and IL-1β in the periodontium were notably reduced after exposure to tFNAs. The alveolar bone was mostly restored to the normal form by tFNAs. The literature indicates that inflammatory factors could activate osteoclastogenesis, enlarge the function of osteoclasts, and restrain the activity of osteoblasts, which would cause excessive bone resorption [44]. Consequently, controlling the inflammatory response of periodontium would reduce the resorption of alveolar bone.

In general, tFNAs cannot only inhibit inflammation and reduce the destruction of periodontal tissue, especially the resorption of the alveolar bone, but can also upregulate the osteogenic differentiation of odontogenic stem cells to promote the formation of new bone under inflammatory conditions. These outcomes indicate that tFNAs could protect periodontal tissue under inflammatory conditions. These findings may provide a basis for the potential applications of tFNA in the biological treatment of periodontitis and in the field of PDLSC-based tissue engineering. In addition, tFNA is regarded as a carrier for the transport of various functionalized groups and drugs, such as antisense peptide nucleic acids, paclitaxel, ethyleneimine, and AS1411 [48,49]. Recent studies have indicated that tFNAs could act as a delivery vehicle and transport the antimicrobial peptide GL13K into some bacteria [50]. Moreover, periodontitis is a subgingival infection triggered by multiple

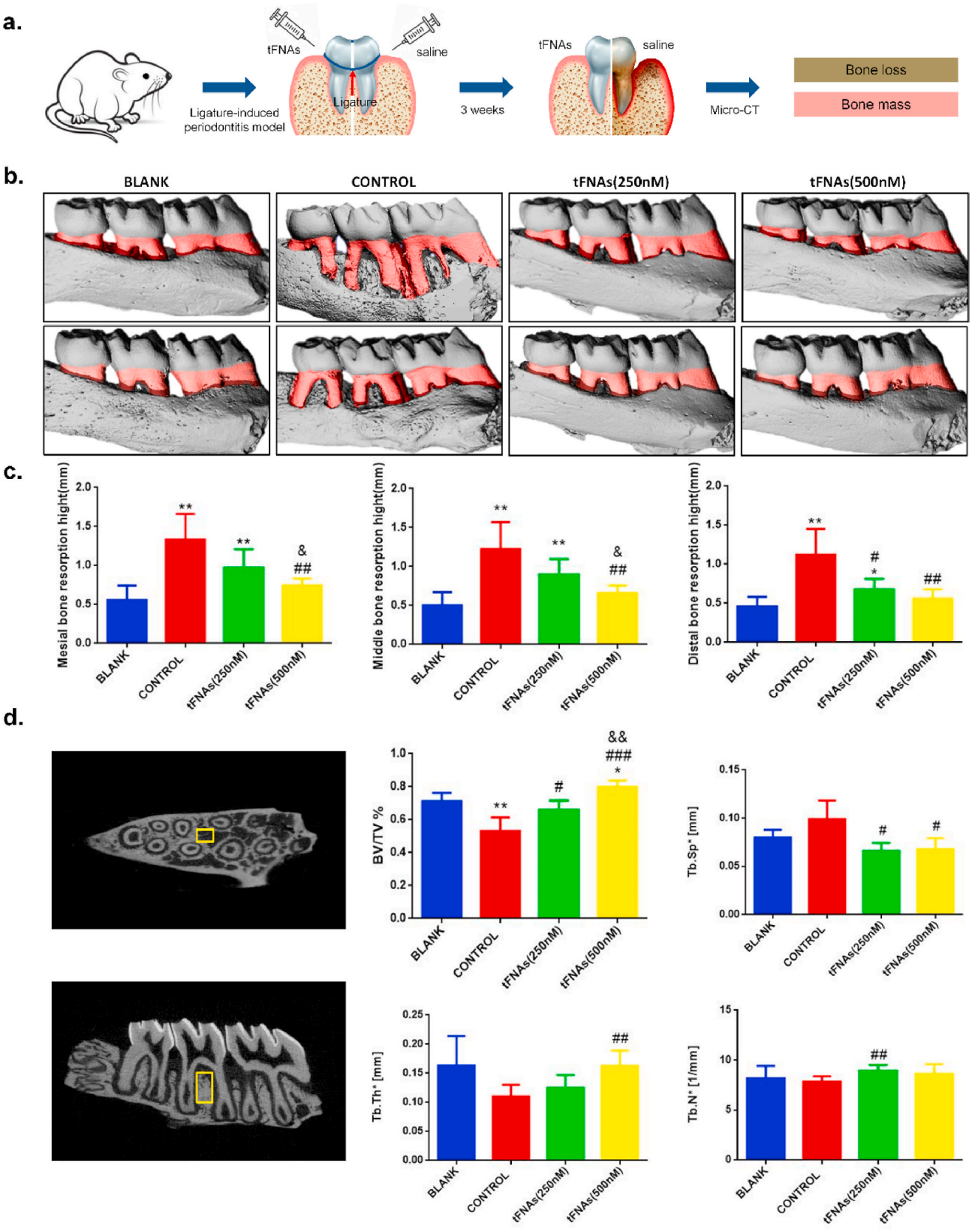

Fig. 7. tFNAs significantly protected the alveolar bone from periodontitis *in vivo*. a. Schematic diagram of the rat periodontitis experiment. b. The micro-CT 3D reconstruction images of left maxillary alveolar bone. The red part displayed the exposure of root. c. Statistical analysis of the mesial, middle, and distal alveolar bone absorption of the second molar (n = 5). *P < 0.5, **P < 0.01, ***P < 0.001 compared with blank group. #P < 0.5, ##P < 0.01, ###P < 0.001 compared with contol group. & P < 0.5 compared with tFNAs (250 nM) group. d. Statistical analysis of the micro-CT results of BV/TV, Tb.N, Tb.Sp and Tb.Th (n = 5). *P < 0.5, **P < 0.01 compared with blank group. #P < 0.5, ##P < 0.01, ###P < 0.001 compared with contol group. && P < 0.5 compared with tFNAs (250 nM) group. The aera marked with yellow line was the region of interest.

bacterial species. Therefore, tFNAs can be used to transport some functional groups to harm specific bacteria. To effectively prevent and treat periodontitis, it is important that future research focuses on strategies that involve the use of compounds that can protect the periodontal tissue and exert antibacterial effects.

5. Conclusion

In conclusion, our study showed that tFNAs could inhibit the release of cellular pro-inflammatory factors such as IL-6, TNF-α, and IL-1β and the production of cellular ROS to facilitate the migration and osteogenic differentiation of PDLSCs *in vitro*. This indicates that tFNAs might have a protective effect on the osteogenic differentiation of PDLSCs under inflammatory conditions. We also found that tFNA inhibited the inflammation of PDLSCs possibly through the MAPK/ERK signaling pathway. In addition, in rat models of periodontitis, tFNAs significantly attenuated inflammatory cell infiltration and greatly downregulated the expression of IL-6 and IL-1β, which inhibited osteoclastogenesis and markedly protect the periodontal tissue including the alveolar bone, cementum and PDL under inflammatory condition. These findings clearly indicated that tFNAs might be adopted as preventive and therapeutic agents against periodontitis.

CRediT authorship contribution statement

Mi Zhou: Conceptualization, Investigation, Methodology, Project administration, Writing - original draft. **Shaojingya Gao:** Data curation, Formal analysis, Investigation, Writing - review & editing. **Xiaolin Zhang:** Methodology, Investigation, Software. **Tianxu Zhang:** Data curation, Methodology, Resources. **Tao Zhang:** Data curation, Investigation, Writing - review & editing. **Taoran Tian:** Data curation, Methodology, Software. **Songhang Li:** Resources, Methodology, Writing - review & editing. **Yunfeng Lin:** Funding acquisition, Supervision, Writing - review & editing. **Xiaoxiao Cai:** Project administration, Funding acquisition, Supervision, Writing - review & editing.

Declaration of competing interest

There is no conflict to declare.

Abbreviations

tFNAs	tetrahedral framework nucleic acids
LPS	lipopolysaccharide
PDLSCs	periodontal ligament stem cells
TEM	transmission electron microscope
ROI	region of interest
BV/TV	the ratio of bone volume to tissue volume
Tb	Th trabecular thickness
Tb.Sp	trabecular separation/space
Tb.N	trabecular number
ROS	reactive oxygen species
FBS	et al. bovine serum
qPCR	quantitative polymerase chain reaction
CEJ	cementoenamel junction
ABC	alveolar bone crest
TRAP	tartrate-resistant acid phosphatase
H&E	hematoxylin and eosin
PFA	polytetrafluoroethylene
EDTA	ethylenediamine tetraacetic acid
DNA	deoxyribonucleic acid
TM	Tris-maleate
PBS	phosphate-buffered saline
ASCs	adipose derived stem cells
DPSCs	dental pulp stem cells
PAGE	polyacrylamide gel electrophoresis
RUNX2	runt-related transcription factor 2
ALP	alkaline phosphate
OPN	osteopontin
IL	interleukin
TNF	tumor necrosis factor
FITC	fluorescein isothiocyanate
Cy-5	Cyanine-5 ssDNA single-stranded DNA; Micro-CT micro-computed tomography
ERK	extracellular signal regulated kinase
JNK	c-jun N-terminal activated protein kinase; MAPK mitogen activated protein kinase

Funding

This study was supported by National Key R&D Program of China (2019YFA0110600) and National Natural Science Foundation of China (81970986, 81771125).

Data statement

The data that support the findings of this study are available from the corresponding author upon reasonable request.

References

[1] B.L. Pihlstrom, B.S. Michalowicz, N.W. Johnson, Periodontal diseases, Lancet 366 (2005) 1809–1820, https://doi.org/10.1016/s0140-6736(05)67728-8.
[2] H. Yamada, T. Nakajima, H. Domon, T. Honda, K. Yamazaki, Endoplasmic reticulum stress response and bone loss in experimental periodontitis in mice, J. Periodontal. Res. 50 (2015) 500–508, https://doi.org/10.1111/jre.12232.
[3] F. Graziani, G. Tsakos, Patient-based outcomes and quality of life, Periodontol 83 (2000) 277–294, https://doi.org/10.1111/prd.12305, 2020.
[4] X. Li, K.M. Kolltveit, L. Tronstad, I. Olsen, Systemic diseases caused by oral infection, Clin. Microbiol. Rev. 13 (2000) 547–558, https://doi.org/10.1128/cmr.13.4.547-558.2000.
[5] N.A. Hickey, L. Shalamanova, K.A. Whitehead, N. Dempsey-Hibbert, C. van der Gast, R.L. Taylor, Exploring the putative interactions between chronic kidney disease and chronic periodontitis, vol. 46, 2020, pp. 61–77, https://doi.org/10.1080/1040841x.2020.1724872.
[6] R.J. Genco, T.E. Van Dyke, Prevention: reducing the risk of CVD in patients with periodontitis, Nat. Rev. Cardiol. 7 (2010) 479–480, https://doi.org/10.1038/nrcardio.2010.120.
[7] S.E. Choi, C. Sima, A. Pandya, Impact of treating oral disease on preventing vascular diseases: a model-based cost-effectiveness analysis of periodontal treatment among patients with type 2 diabetes, Diabetes Care 43 (2020) 563–571, https://doi.org/10.2337/dc19-1201.
[8] G. Hajishengallis, J.D. Lambris, Complement-targeted therapeutics in periodontitis, Adv. Exp. Med. Biol. 735 (2013) 197–206, https://doi.org/10.1007/978-1-4614-4118-2_13.
[9] M.C. Bottino, V. Thomas, G. Schmidt, Y.K. Vohra, T.M. Chu, M.J. Kowolik, G. M. Janowski, Recent advances in the development of GTR/GBR membranes for periodontal regeneration-a materials perspective, Dent. Mater. 28 (2012) 703–721, https://doi.org/10.1016/j.dental.2012.04.022.
[10] P.M. Bartold, S. Gronthos, S. Ivanovski, A. Fisher, D.W. Hutmacher, Tissue engineered periodontal products, J. Periodontal. Res. 51 (2016) 1–15, https://doi.org/10.1111/jre.12275.
[11] F.M. Chen, Y. Jin, Periodontal tissue engineering and regeneration: current approaches and expanding opportunities, Tissue Eng. B Rev. 16 (2010) 219–255, https://doi.org/10.1089/ten.TEB.2009.0562.
[12] K. Chatzivasileiou, K. Kriebel, G. Steinhoff, B. Kreikemeyer, H. Lang, Do oral bacteria alter the regenerative potential of stem cells? A concise review, J. Cell Mol. Med. 19 (2015) 2067–2074, https://doi.org/10.1111/jcmm.12613.
[13] H. Kato, Y. Taguchi, K. Tominaga, M. Umeda, A. Tanaka, Porphyromonas gingivalis LPS inhibits osteoblastic differentiation and promotes pro-inflammatory cytokine production in human periodontal ligament stem cells, Arch. Oral Biol. 59 (2014) 167–175, https://doi.org/10.1016/j.archoralbio.2013.11.008.
[14] T. Kukolj, D. Trivanović, Lipopolysaccharide can modify differentiation and immunomodulatory potential of periodontal ligament stem cells via ERK1,2 signaling, J. Cell. Physiol. 233 (2018) 447–462, https://doi.org/10.1002/jcp.25904.
[15] X. Kong, Y. Liu, R. Ye, B. Zhu, Y. Zhu, X. Liu, C. Hu, H. Luo, Y. Zhang, Y. Ding, Y. Jin, GSK3beta is a checkpoint for TNF-alpha-mediated impaired osteogenic differentiation of mesenchymal stem cells in inflammatory microenvironments, Biochim. Biophys. Acta 1830 (2013) 5119–5129, https://doi.org/10.1016/j.bbagen.2013.07.027.
[16] E. Schilling, R. Weiss, A. Grahnert, M. Bitar, U. Sack, S. Hauschildt, Molecular mechanism of LPS-induced TNF-alpha biosynthesis in polarized human

macrophages, Mol. Immunol. 93 (2018) 206–215, https://doi.org/10.1016/j.molimm.2017.11.026.
[17] T. Nakashima, Y. Kobayashi, S. Yamasaki, A. Kawakami, K. Eguchi, H. Sasaki, H. Sakai, Protein expression and functional difference of membrane-bound and soluble receptor activator of NF-kappaB ligand: modulation of the expression by osteotrophic factors and cytokines, Biochem. Biophys. Res. Commun. 275 (2000) 768–775, https://doi.org/10.1006/bbrc.2000.3379.
[18] Z. Li, B. Zhao, D. Wang, Y. Wen, G. Liu, H. Dong, S. Song, C. Fan, DNA nanostructure-based universal microarray platform for high-efficiency multiplex bioanalysis in biofluids, ACS Appl. Mater. Interfaces 6 (2014) 17944–17953, https://doi.org/10.1021/am5047735.
[19] Y. Wen, H. Pei, Y. Shen, J. Xi, M. Lin, N. Lu, X. Shen, J. Li, C. Fan, DNA Nanostructure-based Interfacial engineering for PCR-free ultrasensitive electrochemical analysis of microRNA, Sci. Rep. 2 (2012) 867, https://doi.org/10.1038/srep00867.
[20] A.S. Walsh, H. Yin, C.M. Erben, M.J. Wood, A.J. Turberfield, DNA cage delivery to mammalian cells, ACS Nano 5 (2011) 5427–5432, https://doi.org/10.1021/nn2005574.
[21] P. Charoenphol, H. Bermudez, Aptamer-targeted DNA nanostructures for therapeutic delivery, Mol. Pharm. 11 (2014) 1721–1725, https://doi.org/10.1021/mp500047b.
[22] S. Shi, Q. Peng, X. Shao, J. Xie, S. Lin, T. Zhang, Q. Li, X. Li, Y. Lin, Self-assembled tetrahedral DNA nanostructures promote adipose-derived stem cell migration via lncRNA XLOC 010623 and RHOA/ROCK2 signal pathway, ACS Appl. Mater. Interfaces 8 (2016) 19353–19363, https://doi.org/10.1021/acsami.6b06528.
[23] W. Ma, X. Shao, D. Zhao, Q. Li, M. Liu, T. Zhou, X. Xie, C. Mao, Y. Zhang, Y. Lin, Self-assembled tetrahedral DNA nanostructures promote neural stem cell proliferation and neuronal differentiation, vol. 10, 2018, pp. 7892–7900, https://doi.org/10.1021/acsami.8b00833.
[24] M. Zhou, N.X. Liu, S.R. Shi, Y. Li, Q. Zhang, Q.Q. Ma, T.R. Tian, W.J. Ma, X.X. Cai, Y.F. Lin, Effect of tetrahedral DNA nanostructures on proliferation and osteo/odontogenic differentiation of dental pulp stem cells via activation of the notch signaling pathway, Nanomedicine 14 (2018) 1227–1236, https://doi.org/10.1016/j.nano.2018.02.004.
[25] M. Zhou, N. Liu, Q. Zhang, T. Tian, Q. Ma, T. Zhang, X. Cai, Effect of Tetrahedral DNA Nanostructures on Proliferation and Osteogenic Differentiation of Human Periodontal Ligament Stem Cells, vol. 52, 2019, e12566, https://doi.org/10.1111/cpr.12566.
[26] Q. Zhang, S. Lin, S. Shi, T. Zhang, Q. Ma, T. Tian, T. Zhou, X. Cai, Y. Lin, Anti-inflammatory and antioxidative effects of tetrahedral DNA nanostructures via the modulation of macrophage responses, vol. 10, 2018, pp. 3421–3430, https://doi.org/10.1021/acsami.7b17928.
[27] E.K. Kim, E.J. Choi, Pathological roles of MAPK signaling pathways in human diseases, Biochim. Biophys. Acta 1802 (2010) 396–405, https://doi.org/10.1016/j.bbadis.2009.12.009.
[28] D. Zhao, M. Liu, Q. Li, X. Zhang, C. Xue, Y. Lin, Tetrahedral DNA nanostructure promotes endothelial cell proliferation, migration, and angiogenesis via Notch signaling pathway, ACS Appl. Mater. Interfaces 10 (2018) 37911–37918, https://doi.org/10.1021/acsami.8b16518.
[29] X. Qin, N. Li, M. Zhang, S. Lin, J. Zhu, D. Xiao, W. Cui, T. Zhang, Y. Lin, Tetrahedral framework nucleic acids prevent retina ischemia-reperfusion injury from oxidative stress via activating the Akt/Nrf 2 pathway, Nanoscale 11 (2019) 20667–20675, https://doi.org/10.1039/c9nr07171g.
[30] Y. He, Y. Zhong, Y. Su, Y. Lu, Z. Jiang, F. Peng, T. Xu, S. Su, Q. Huang, C. Fan, S. T. Lee, Water-dispersed near-infrared-emitting quantum dots of ultrasmall sizes for in vitro and in vivo imaging, Angew Chem. Int. Ed. Engl. 50 (2011) 5695–5698, https://doi.org/10.1002/anie.201004398.
[31] T. Tian, J. Liao, T. Zhou, S. Lin, T. Zhang, S.R. Shi, X. Cai, Y. Lin, Fabrication of calcium phosphate microflowers and their extended application in bone regeneration, ACS Appl. Mater. Interfaces 9 (2017) 30437–30447, https://doi.org/10.1021/acsami.7b09176.
[32] N. Liu, M. Zhou, Q. Zhang, L. Yong, T. Zhang, T. Tian, Q. Ma, S. Lin, B. Zhu, X. Cai, Effect of substrate stiffness on proliferation and differentiation of periodontal ligament stem cells, Cell Prolif 51 (2018), e12478, https://doi.org/10.1111/cpr.12478.
[33] N. Yang, Y. Li, G. Wang, Y. Ding, Y. Jin, Y. Xu, Tumor necrosis factor-α suppresses adipogenic and osteogenic differentiation of human periodontal ligament stem cell by inhibiting miR-21/Spry 1 functional axis, Differentiation 97 (2017) 33–43, https://doi.org/10.1016/j.diff.2017.08.004.
[34] D. Zhao, Q. Li, M. Liu, W. Ma, T. Zhou, C. Xue, X. Cai, Substrate stiffness regulated migration and invasion ability of adenoid cystic carcinoma cells via RhoA/ROCK pathway, Cell Prolif 51 (2018), e12442, https://doi.org/10.1111/cpr.12442.
[35] J. Shin, T. Maekawa, T. Abe, E. Hajishengallis, K. Hosur, K. Pyaram, I. Mitroulis, T. Chavakis, G. Hajishengallis, DEL-1 restrains osteoclastogenesis and inhibits inflammatory bone loss in nonhuman primates, Sci. Transl. Med. 7 (2015), https://doi.org/10.1126/scitranslmed.aac5380, 307ra155.
[36] M. Zhang, J. Zhu, X. Qin, M. Zhou, X. Zhang, Y. Gao, T. Zhang, D. Xiao, W. Cui, X. Cai, Cardioprotection of tetrahedral DNA nanostructures in myocardial ischemia-reperfusion injury, ACS Appl. Mater. Interfaces 11 (2019) 30631–30639, https://doi.org/10.1021/acsami.9b10645.
[37] W. Cui, Y. Zhan, X. Shao, W. Fu, D. Xiao, J. Zhu, X. Qin, T. Zhang, M. Zhang, Y. Zhou, Y. Lin, Neuroprotective and neurotherapeutic effects of tetrahedral framework nucleic acids on Parkinson's disease in vitro, ACS Appl. Mater. Interfaces 11 (2019) 32787–32797, https://doi.org/10.1021/acsami.9b10308.
[38] X.R. Shao, S.Y. Lin, Q. Peng, S.R. Shi, X.L. Li, T. Zhang, Y.F. Lin, Effect of tetrahedral DNA nanostructures on osteogenic differentiation of mesenchymal stem cells via activation of the Wnt/β-catenin signaling pathway, Nanomedicine 13 (2017) 1809–1819, https://doi.org/10.1016/j.nano.2017.02.011.
[39] M. Cáp, L. Váchová, Z. Palková, Reactive oxygen species in the signaling and adaptation of multicellular microbial communities, Oxid. Med. Cell. Longev. (2012) 976753, https://doi.org/10.1155/2012/976753, 2012.
[40] Y.S. Hah, H.G. Kang, H.Y. Cho, S.H. Shin, U.K. Kim, B.W. Park, S.I. Lee, G.J. Rho, J. R. Kim, J.H. Byun, JNK signaling plays an important role in the effects of TNF-α and IL-1β on in vitro osteoblastic differentiation of cultured human periosteal-derived cells, Mol. Biol. Rep. 40 (2013) 4869–4881, https://doi.org/10.1007/s11033-013-2586-3.
[41] K. Marupanthorn, C. Tantrawatpan, D. Tantikanlayaporn, P. Kheolamai, S. Manochantr, The effects of TNF-α on osteogenic differentiation of umbilical cord derived mesenchymal stem cells, J. Med. Assoc. Thai. 98 (Suppl 3) (2015) S34–S40.
[42] X. Jin, J. Wang, Z.M. Xia, C.H. Shang, Q.L. Chao, Y.R. Liu, H.Y. Fan, D.Q. Chen, F. Qiu, F. Zhao, Anti-inflammatory and anti-oxidative activities of paeonol and its metabolites through blocking MAPK/ERK/p38 signaling pathway, Inflammation 39 (2016) 434–446, https://doi.org/10.1007/s10753-015-0265-3.
[43] M. Riera-Borrull, V.D. Cuevas, Palmitate conditions macrophages for enhanced responses toward inflammatory stimuli via JNK activation, J. Immunol. 199 (2017) 3858–3869, https://doi.org/10.4049/jimmunol.1700845.
[44] K. Redlich, J.S. Smolen, Inflammatory bone loss: pathogenesis and therapeutic intervention, Nat. Rev. Drug Discov. 11 (2012) 234–250, https://doi.org/10.1038/nrd3669.
[45] M. Padial-Molina, S.L. Volk, H.F. Rios, Periostin increases migration and proliferation of human periodontal ligament fibroblasts challenged by tumor necrosis factor -α and Porphyromonas gingivalis lipopolysaccharides, J. Periodontal. Res. 49 (2014) 405–414, https://doi.org/10.1111/jre.12120.
[46] N. Liu, X. Zhang, N. Li, M. Zhou, T. Zhang, S. Li, X. Cai, P. Ji, Y. Lin, Tetrahedral framework nucleic acids promote corneal epithelial wound healing in vitro and in vivo, Small 15 (2019), e1901907, https://doi.org/10.1002/smll.201901907.
[47] C. Mao, W. Pan, X. Shao, W. Ma, Y. Zhang, Y. Zhan, Y. Gao, Y. Lin, The Clearance Effect of Tetrahedral DNA Nanostructures on Senescent Human Dermal Fibroblasts, vol. 11, 2019, pp. 1942–1950, https://doi.org/10.1021/acsami.8b20530.
[48] T. Tian, T. Zhang, T. Zhou, S. Lin, S. Shi, Y. Lin, Synthesis of an ethyleneimine/tetrahedral DNA nanostructure complex and its potential application as a multi-functional delivery vehicle, Nanoscale 9 (2017) 18402–18412, https://doi.org/10.1039/c7nr07130b.
[49] Q. Li, D. Zhao, X. Shao, S. Lin, X. Xie, M. Liu, W. Ma, S. Shi, Y. Lin, Aptamer-modified tetrahedral DNA nanostructure for tumor-targeted drug delivery, vol. 9, 2017, pp. 36695–36701, https://doi.org/10.1021/acsami.7b13328.
[50] Y. Liu, Y. Sun, S. Li, M. Liu, X. Qin, X. Chen, Y. Lin, Tetrahedral framework nucleic acids deliver antimicrobial peptides with improved effects and less susceptibility to bacterial degradation, Nano Lett. 20 (2020) 3602–3610, https://doi.org/10.1021/acs.nanolett.0c00529.